

Homogeneous nucleation in ${}^4\text{He}$: A corresponding-states analysis

Dipen N. Sinha

Los Alamos National Laboratory, University of California, Los Alamos, New Mexico 87545

J. S. Semura and L. C. Brodie

*Department of Physics/Environmental Sciences and Resources Program,
Portland State University, Portland, Oregon 97207*

(Received 4 January 1982)

We report homogeneous-nucleation-temperature measurements in liquid ${}^4\text{He}$ over a bath-temperature range $2.31 < T_b < 4.62$ K. These measurements were performed with the use of a transient superheating technique. The nucleation data constitute a demonstration of the quantitative accuracy of the Becker-Döring nucleation theory in describing the first-order transition kinetics in a quantum liquid, such as liquid ${}^4\text{He}$, in a region far from the critical point. A simple empirical form is presented for estimating the homogeneous-nucleation temperatures for any liquid with a spherically symmetric interatomic potential. The ${}^4\text{He}$ data are compared with nucleation data for Ar, Kr, Xe, and H_2 ; theoretical predictions for ${}^3\text{He}$ are given in terms of reduced quantities. It is shown that the nucleation data for both quantum and classical liquids obey a quantum law of corresponding states (QCS). On the basis of this QCS analysis, predictions of homogeneous-nucleation temperatures are made for hydrogen isotopes such as HD, DT, HT, and T_2 .

I. INTRODUCTION

The problem of nucleated phase changes in metastable fluids has been an active area of study for many years. Such phase transitions are associated with the existence of a thermodynamic barrier to the formation of droplets of a second phase in a homogeneous metastable parent phase. The so-called "classical" nucleation theories, such as that of Becker and Döring (BD),^{1,2} generally consider the rate of phase transformation of metastable states as a function of the degree of metastability, which can be defined by the superheating or the supercooling of the liquid. The predicted rate varies by several orders of magnitude within a narrow range of superheating (or supercooling) of a liquid, thus effectively defining a kinetic limit of metastability. This is the limit measured experimentally and is commonly referred to as the homogeneous nucleation limit or homogeneous nucleation temperature, in the case of superheated liquids.

Much of the recent work in nucleation has been focused on studying near-critical fluids,³⁻¹⁴ including both one-component systems and binary mixtures. Without exception, the experimental results have appeared to be in dramatic disagreement with conventionally interpreted nucleation-rate formulas. Recent theoretical ideas^{11,12} offer a resolution of this discrepancy by pointing out that the experi-

mentally meaningful quantity is not the nucleation rate itself, but the time required for the reaction to go to completion. Near the critical point, overall reaction rates are likely to be appreciably different from estimates based on nucleation alone.

In contrast to the case of near-critical fluids, homogeneous nucleation measurements carried out in a number of superheated organic¹⁵ and cryogenic liquids,¹⁶ *far from the critical region*, indicate excellent agreement between experiment and Becker-Döring theory. Whether one should also expect such an agreement in the case of quantum systems, such as liquids ${}^3\text{He}$ and ${}^4\text{He}$, has remained an open question. Dahl and Moldover⁷ have studied the lifetime of superheated metastable states in liquid ${}^3\text{He}$ near the critical point. Although their limited data are apparently consistent with other measurements in near-critical nonquantum liquids and binary mixtures,¹³ nothing definitive can be concluded from this regarding the validity of the classical nucleation theories in the case of quantum liquids far from the critical region. In different experiments, such as tensile strength measurements^{17,18} in ${}^4\text{He}$, anomalously low values have been observed, contrary to theoretical predictions. It has been speculated in this connection,^{17,18} that such disagreement with theory could arise because conventional nucleation theory might be inappropriate for all helium liquids, since in these liquids the

quantum-mechanical zero-point energy per atom is significant in comparison to kT , the atom's thermal energy. It is possible that an essentially different nucleation mechanism is involved, quantum rather than thermal, as was first proposed by Lifshitz and Kagan.¹⁹

The central purpose of this paper is to address the question of the applicability of conventional nucleation theories to the case of a quantum system, such as the helium liquids. We present here detailed experimental results on nucleation in superheated *normal* liquid ${}^4\text{He}$, far from the critical region, that are in excellent quantitative agreement with the predictions of classical (BD) theory of homogeneous nucleation. The experimental technique we employed involves the fast superheating of a thin layer of liquid helium in contact with an electrically step-pulse heated single crystal of bismuth.

A second purpose of this paper is to present a systemization of the homogeneous-nucleation-temperature measurements available for the condensed noble gases. We therefore make use of our ${}^4\text{He}$ measurements along with data of others for Ar, Kr, and Xe, as well as H_2 , to analyze the available data and to formulate an empirically derived law of corresponding states for the homogeneous nucleation temperature.

We should make a point concerning the terminology. The phrase "classical nucleation theory" has become accepted in reference to the Becker-Döring class of theories and we will follow this usage in this paper. However, the word classical as used in the above phrase does *not* mean "nonquantum mechanical." Hence classical nucleation theory can remain valid for nucleated phase transitions in quantum liquids. More specifically, one would expect that, since the derivation of BD and of more recent nucleation theories rests primarily on kinetic equations that make no specific reference to either *classical* mechanics or *quantum* mechanics, these theories should remain valid for the quantum liquids *whenever the nucleative driving force is the thermal activation of nuclei over the energy barrier.*

In Sec. II, we present a brief discussion of the classical nucleation theory and its limit of applicability involving nucleation due to quantum tunneling through the thermodynamic barrier at very low temperatures. The experimental details of the transient superheating technique are described in Sec. III, and the experimental observations are presented in Sec. IV. In Sec. V, we discuss in detail the interpretations of the experimental observations. A series of arguments is presented to support our

claim that the experimental data do indeed provide measurements of the homogeneous nucleation temperature in liquid ${}^4\text{He}$. In Sec. VI, the experimental results are discussed. The excellent agreement between our experimental data and the predictions from classical nucleation theory suggests that within our range of measurements no new mechanism for nucleation, e.g., quantum tunneling, need be invoked to explain the liquid-to-vapor nucleative phase transition in a quantum system. In Sec. VII, we compare our ${}^4\text{He}$ data with nucleation data in condensed noble gases, such as Ar, Kr, and Xe, as well as with H_2 . These data are further examined from the viewpoint of corresponding states. On the basis of such a corresponding-states analysis, predictions of the homogeneous-nucleation temperature are made for several hydrogen isotopes. Section VIII is devoted to a brief summary.

II. THEORETICAL BACKGROUND

In the classical nucleation theories, the formation of critical-size nuclei in the metastable (superheated) liquid as a result of thermal heterophase fluctuations is described in terms of a *thermally activated* transition across a thermodynamic energy barrier. The height of this energy barrier is determined by the minimum work of formation W_{cr} of a critical (vapor-filled) nucleus. The rate of formation of such critical nuclei is generally described by an Arrhenius-type expression:

$$J = J_0 \exp(-W_{\text{cr}}/kT), \quad (1)$$

where J_0 is an attempt frequency determined by the thermophysical properties of the liquid and by the dynamics of the nucleus formation process, T is the temperature, and k is the Boltzmann constant. In terms of the thermophysical properties of the liquid, Eq. (1) can be expressed more completely as¹⁵

$$J = N \left[\frac{2\gamma}{\pi m B} \right]^{1/2} \exp \left[- \frac{16\pi\gamma^3}{3kT(P_e - P_l)^2\delta^2} \right], \quad (2)$$

where J is the rate of formation of critical nuclei per unit volume per unit time, γ is the bulk surface tension, N is the molecular number density of the liquid, m is the molecular mass, B is a constant ($B \simeq \frac{2}{3}$), P_e is the equilibrium vapor pressure, and P_l is the ambient pressure. The Poynting correction factor δ relates P_v , the vapor pressure of the liquid

under an ambient pressure P_l , to the equilibrium pressure: $\delta = (P_v - P_l)/(P_e - P_l)$. In a narrow range of superheating, the nucleation rate is extremely sensitive to a small change in temperature. For example, in the case of liquid ^4He at atmospheric pressure, some 12 orders of magnitude variation in the J value corresponds to a 1% change in T . Thus, an effective homogeneous-nucleation temperature T_h can be defined. The kinetic coefficient in the preexponential factor of Eq. (2) does not include the modifications due to viscous and inertial forces that affect the dynamics of nuclei growth. Following Kagan's prescription,²⁰ our estimate of the effects of these factors shows them to be negligible in determining the homogeneous-nucleation temperature in liquid ^4He .

The rate expression given by Eq. (2) describes steady-state nucleation. Under non-steady-state conditions, such as the transient superheating of a liquid, Eq. (2) should be modified to include a time characterizing the relaxation to a steady state. Such relaxation rates have been reviewed by Abraham.²¹ We use the form

$$J(t) = J[1 - \exp(-t/\tau_s)] , \quad (3)$$

where J is the steady-state nucleation rate, and τ_s is the characteristic relaxation time for the establishment of steady-state nucleation. Our estimate of the relaxation time for superheated liquid ^4He over a wide range of bath temperatures shows τ_s to be extremely short, varying roughly between 2 and 10 ns. Since this relaxation time is several orders of magnitude smaller than the time scale involved in our transient superheating experiment (as described in Sec. IV) of 0.1 to 30 ms, $J(t)$ can be set equal to J .

Returning to our earlier discussion of the rate of formation of critical nuclei, we see that Eq. (1) suggests that the rate of classical transitions by thermal activation over the thermodynamic barrier should decrease with decreasing temperature. Thus, the rate of nucleation is predicted to decrease to zero as $T \rightarrow 0$. On the other hand, at very low temperatures in quantum liquids where the de Broglie wavelength exceeds the width of the thermodynamic potential barrier, subbarrier tunneling transitions with the formation of supercritical nuclei in the metastable liquid may become significant. In this case, the probability of through-the-barrier tunneling transitions should level off as $T \rightarrow 0$. Lifshitz and Kagan¹⁹ were the first to consider the problem of quantum tunneling nucleation. Using their model of quantum nucleation, we have estimated a tunneling temperature T^* below which tunneling starts to

dominate exponentially the Arrhenius-type transitions [Eq. (1)]. Our estimates of T^* are $\simeq 0.3$ K for ^4He and $\simeq 0.2$ K for ^3He . We emphasize that such tunneling nucleation cannot be observed in an exclusively superheating type of experiment because tunneling is expected to become predominant at negative pressures. However, it should be possible to study such quantum nucleation by means of tensile strength experiments. We estimate that roughly, from the Lifshitz and Kagan model, one can expect to encounter such phenomena below estimated negative pressures of -14.6 atm in ^4He and -5.2 atm in ^3He .

From the above discussion, we conclude that it is quite likely that the conventional BD type of nucleation theory should be adequate in describing liquid-to-vapor homogeneous nucleation in superheated quantum liquids without invoking any new nucleation mechanisms.

III. EXPERIMENTAL

Our investigations involve the electrical step-pulse heating of a single crystal of bismuth immersed in a bath of liquid helium and subjected to a steady magnetic field. A constant electric current is applied at time $t=0$, and the change in crystal magnetoresistance ΔR_B , resulting from the temperature changes ΔT caused by Joule heating, is subsequently observed as a function of time. The ΔT of the crystal is relatively easy to determine because of the strong temperature dependence of magnetoresistance R_B of a high quality single crystal of bismuth at liquid-helium temperatures. Thus, the crystal serves as a heater as well as a sensitive thermometer to measure the temperature of the liquid helium in immediate contact with its surface.

The crystals were grown in the shape of a parallelepiped and were approximately 6 cm long, 1.5 mm thick, and 5 mm wide. They were mounted in micarta holders in a way to maximize exposure to liquid helium and to minimize strain due to differential thermal contraction. The holder was positioned with its long axis vertical at the bottom of a conventional Pyrex double Dewar system, which was located between the pole pieces of an electromagnet. The helium vapor pressure was measured by oil, mercury, and capacitance monometers (Setra System Model No. 204) in different pressure ranges, and the 1958 vapor-pressure scale was used to determine the bath temperature.

The crystal ΔT was determined as a function of time by observing the resulting ΔR_B using a dif-

ferential electronic technique. The variation of magnetoresistance with temperature was approximately linear for ΔT less than 1 K. The temperature sensitivity $S = (1/R_B)(dR_B/dT)$ of the crystal used for these measurements was 0.25 K^{-1} . With proper calibration of the crystal as a thermometer, in terms of its temperature-dependent magnetoresistance, the overall uncertainty in the temperature measurement was approximately $\pm 10 \text{ mK}$, including the effect of Kapitza resistance. The response time of the bismuth crystal transient thermometer was less than $100 \mu\text{s}$, so the temperature changes that were on a millisecond time scale were adequately reproduced. Complete details of the bismuth thermometer and the associated electronic circuitry can be found in previous publications.^{22,23}

We have found that liquid helium in contact with the surface of a bismuth crystal heater thermometer can be superheated up to its homogeneous nucleation temperature by applying a step-pulse electric current to the crystal. Such superheating becomes possible primarily due to the finite delay time (30–100 ms) involved in the inception of heterogeneous nucleation at the solid-liquid interface. Therefore, if the heating rate is sufficiently high, the homogeneous nucleation limit is reached before appreciable heterogeneous nucleation can take place. The existence of such a delay time in cryogenic liquids has been reported previously.²⁴ The delay time, particularly in liquid helium, is due to its excellent wettability which makes the presence of vapor-filled sites on a submerged solid surface very unlikely. Moreover, at such low temperatures any dissolved impurity gases will be frozen. Consequently, under transient heating conditions, in the initial periods, the superheating of the liquid in contact with the heater surface is entirely due to thermal conduction. Heterogeneous nucleation does not occur until an appropriate superheat temperature and thermal boundary conditions are reached.²⁵ These points will be discussed in greater detail in Sec. V. A similar pulse-heating technique was first used by Skripov and co-workers²⁶ to study the homogeneous-nucleation limit in several organic liquids.

IV. OBSERVATIONS

Typical superheat temperature ΔT -vs-time (t) curves are shown in Figs. 1(a) and 1(b) for several values of p , the applied power per unit area of the solid's surface. The ΔT -vs- t curves initially rise above, i.e., *overshoot*, their steady-state values.

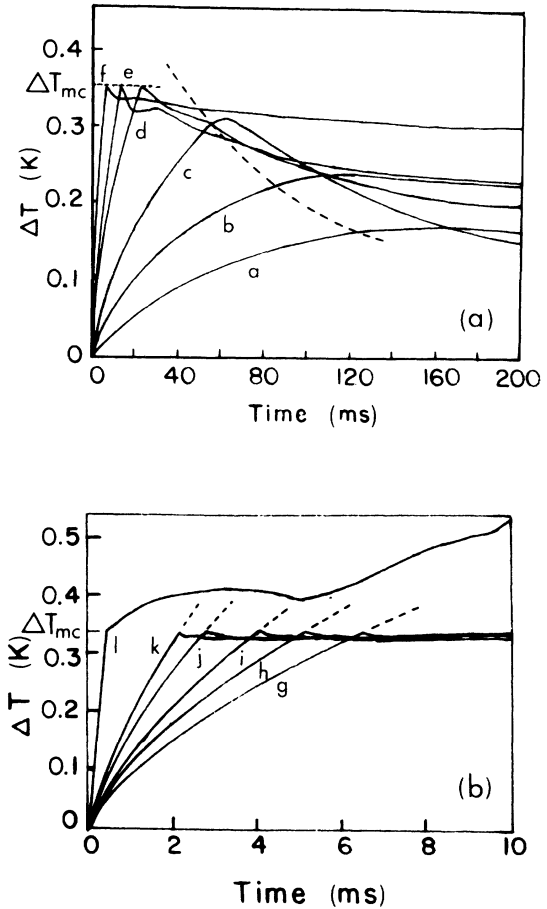


FIG. 1. Superheat temperature ΔT vs time. Transient superheat temperature curves are shown for a range of low and high applied powers per unit area. The bath temperature is 4.2 K. The letters labeling each curve represents the applied power per unit area in mW/cm^2 : (a) 5, (b) 9, (c) 15, (d) 29, (e) 41, (f) 72, (g) 58, (h) 70, (i) 80, (j) 106, (k) 127, (l) 430 mW/cm^2 .

Each curve subsequently cools toward its steady-state value after attaining a maximum superheat temperature ΔT_m . For the relatively lower range of values of p [Fig. 1(a)] the temperature overshoots appear to be smoothly rounded in nature. As p is increased, the maximum superheat temperature ΔT_m of these overshoots becomes greater in magnitude and occurs at increasingly earlier times.

At somewhat higher values of p , typically above $30 \text{ mW}/\text{cm}^2$, the temperature overshoots have two distinct characteristics: (1) the transient superheat temperature curves develop quite sharp peaks at the maximum temperature, and (2) the maximum superheat temperature ΔT_m becomes a constant ΔT_{mc} (within about 5 mK, the resolution of our experiment), independent of p . Figure 1(b) shows signifi-

cantly higher power transient curves and much shorter time scales. [The significance of the dashed curves in Figs. 1(a) and 1(b) is discussed in Sec. V.] The constancy of the maximum overshoot temperature is illustrated in Fig. 2, where ΔT_m is plotted as a function of the applied power for several values of the initial helium bath temperature T_b . For example, at $T_b = 4.2$ K, ΔT_m is constant for p greater than approximately 35 mW/cm^2 up to the maximum value used, roughly 420 mW/cm^2 (Fig. 2 only shows data up to a maximum of 120 mW/cm^2). At each bath temperature, the portion of the curves in Fig. 2 for which ΔT_m is constant corresponds to a sharp peak in the overshoots on a ΔT -vs- t plot. Note also in Fig. 2 that ΔT_{mc} increases with decreasing bath temperature.

At significantly higher powers, roughly above 400 mW/cm^2 , the sharp peak in the overshoot takes the shape of a kink, and the temperature beyond that continually rises toward a steady film foiling condition. These kinks are found to be at the same superheat ΔT_{mc} as the sharp peaks at any given bath temperature [Fig. 1(b)]. The lowest bath temperature at which the above behavior in the transient temperature response could be observed is the superfluid transition temperature. Although it is not shown in Fig. 2, as the bath temperature is

lowered through the λ point, all indications of superheating decrease by several orders of magnitude and the overshoots disappear. Because of the high thermal conductivity of superfluid helium, superheating of the liquid was not possible with the low powers used in our experiment. Presumably, using much larger values of p and smaller volume of liquid, this technique could be extended to bath temperatures below the λ point. (Recently, Rybarcyk and Tough²⁷ have succeeded in superheating superfluid ^4He employing a different experimental approach.) The upper bath-temperature limit in our experiment was limited to approximately 4.6 K because of the risk involved in pressurizing the glass Dewar beyond 1.25 atm.

V. INTERPRETATION OF EXPERIMENTAL OBSERVATIONS

In this section, we justify our interpretation of the sharp breaks in the transient temperature overshoots as resulting from the onset of homogeneous nucleation. We propose that the temperature overshoots in the ΔT -vs- t curves result from a time delay τ in the onset of heterogeneous nucleation. In the initial stages of heating, the liquid helium in

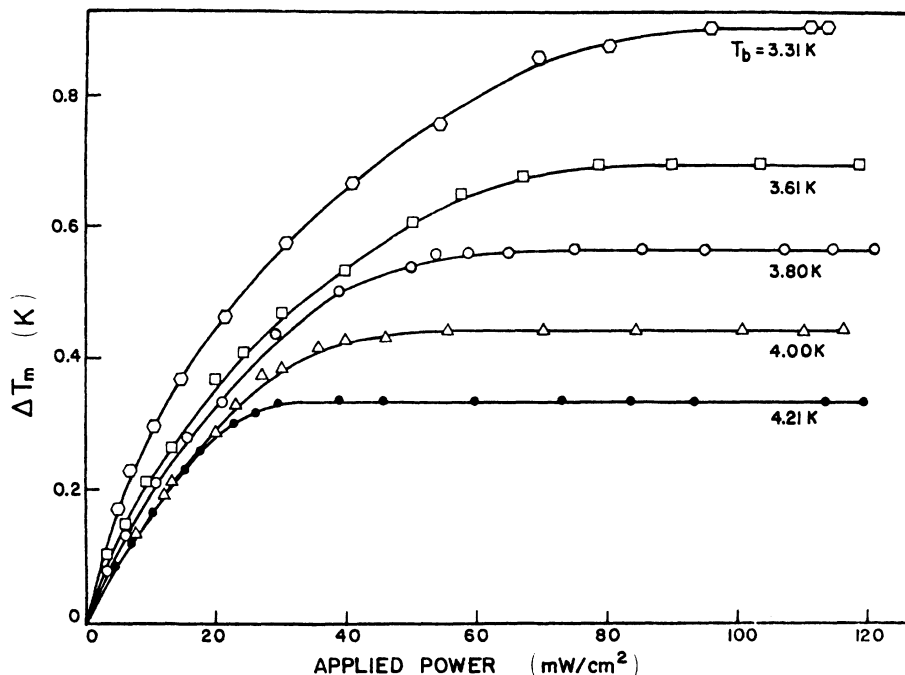


FIG. 2. Maximum superheat temperature as a function of applied power. Maximum superheat temperature ΔT_m is plotted as a function of applied power per unit area p for several initial ^4He bath temperatures. For each temperature ΔT_m approaches a constant value ΔT_{mc} as p increases.

contact with the heater surface is superheated primarily by thermal conduction. For lower values of p , activation of nucleation sites begins at an appropriate superheat temperature, depending on the heating rate and the surface condition of the heater. Heterogeneous nucleation then proceeds at a relatively gradual rate because the potential nucleation sites consisting of crystal surface irregularities are randomly distributed in size, shape, and number density per unit surface area. The rounded overshoots, observed at lower values of p , are the result. On the other hand, at higher applied powers, approximately above 30 mW/cm^2 , the rate of heating is faster and the superheat of the liquid helium layer adjacent to the heater surface reaches the homogeneous nucleation temperature before appreciable heterogeneous nucleation at the solid-liquid interface can prevent it from doing so. Thus, the sharp peaks in the overshoots that occur at a constant superheat temperature ΔT_{mc} result from a very rapid onset of homogeneous nucleation in the superheated liquid-helium layer. The maximum temperature gradient in the thermal boundary layer corresponding to applied powers in the range of interest is estimated²⁸ to be of the order of 20 mK per micron, and, consequently, the temperature difference across a critical-size nucleus of approximately $100\text{-}\text{\AA}$ diameter would be only about 0.2 mK . Thus, the temperature gradients across critical nuclei are much smaller than the quoted overall uncertainty in our experimental measurement of $\pm 10 \text{ mK}$.

Because it may at first seem surprising that the homogeneous-nucleation limit can be attained by heating a solid in a liquid, we present the reasons for our interpretation of the sharp temperature peaks as being due to homogeneous nucleation. We cite the following eight arguments in support of this claim.

(1) Due to the excellent wettability (the liquid-solid contact angle is near zero) and low surface tension of liquid helium, the presence of vapor-filled surface cavities is unlikely. Moreover, the low temperatures involved preclude impurity gases from being inside the cavities. Consequently, in the initial stages of superheating there are no active nucleation sites on the solid surface to start with and the superheating of the liquid helium takes place solely due to thermal conduction from the heater into the liquid. This fact is confirmed by the excellent agreement between the observed superheat temperature in the initial stages of heating and predictions based on the assumption that heat is removed from the solid surface by thermal conduction into

the liquid.²⁸ Figure 1(b) shows the typical excellent agreement of the temperature response predicted from the conduction assumption (dashed lines associated with curves g through k) with the observed transient superheat temperature (solid lines prior to the sharp peaks). In Fig. 1(a), the dashed curve represents the locus of the points marking the instances at which the measured temperature response is observed to begin deviating from the predicted temperature response according to the thermal conduction assumption. Such deviation in the temperature response is caused by the additional heat transport due to convection and heterogeneous nucleation. Thus, the dashed curve [Fig. 1(a)] represents the locus of the effective delay time τ to onset of convection and heterogeneous nucleation. If the superheating takes place on a time scale less than τ , the liquid can be superheated up to the homogeneous nucleation temperature by thermal conduction without significant competition from heterogeneous nucleation. The agreement between the observed temperature response up to the sharp peaks and the predictions from the conduction hypothesis (dashed lines associated with curves g through k) shown in Fig. 1(b) supports this assumption that, in time scales $t < \tau$, heterogeneous nucleation is not likely to be significant in the superheating process.

(2) The *abrupt change* in the characteristics of the temperature overshoots from rounded to sharp peaks as the heating rate is increased strongly suggests that two different processes are involved. The fact that the sharp peaks occur only at times less than τ , is an indication that the sharp peaks are caused by a sudden onset of homogeneous nucleation in a thin superheated layer of liquid helium. We believe the sudden drop in temperature associated with the sharp peak to be due to extraction of thermal energy from the heater surface for growth of the critical nuclei formed in the process of homogeneous nucleation.

(3) The sharp peaks in the temperature overshoots occur at a *constant* superheat temperature ΔT_{mc} , independent of applied power. In our first argument we show evidence that up to the development of the sharp peaks, heterogeneous nucleation is not involved. The characteristic constant superheat associated with the sharp peaks further supports our argument because it is highly unlikely that a process such as heterogeneous nucleation could produce a temperature pattern with such reproducibility and independence of the applied power. On the other hand, the probability of homogeneous nucleation

becomes significant only above a narrowly defined superheat temperature range and the resulting nucleation process is extremely rapid. The value ΔT_{mc} has been reproduced at any given bath temperature with different bismuth crystals of varied surface conditions, using both an electropolished surface and surfaces filled with etch pits. The lack of influence of the surface microgeometry on ΔT_{mc} is further evidence that the sharp peaks are not due to a sudden onset of heterogeneous nucleation. In contrast, the homogeneous nucleation temperature is a characteristic property of the liquid only and does not depend on the microgeometry of the solid surface.

(4) We found that once nucleation takes place on the surface, it takes several seconds before the nucleation sites are deactivated, i.e., become refilled with liquid helium. If the heating current is turned back on before that time, the effects of preexisting active nucleation sites can be clearly observed. Such effects manifest themselves through the lowering of the peak superheat temperatures of the rounded overshoots at any given applied power. The effects can also be observed in the case of those sharp peaks associated with relatively lower power values (around 30–40 mW/cm² at atmospheric pressure). Fast repeated pulsing tends to make these sharp peaks rounded. However, at higher power values, the influence of the preexisting active nucleation sites is of diminishing importance. This can be inferred from the fact that the higher power sharp peaks are not affected and the original characteristic constant superheat ΔT_{mc} associated with such sharp peaks can still be observed. The only difference in the case of preexisting active nucleation sites is that the ΔT_m -vs- p characteristics shown in Fig. 2 are shifted slightly toward higher powers. This result is consistent with that of the pulse heating method²⁶ used in organic liquids in which it was observed that at high heating rates, attainment of homogeneous nucleation temperature is possible even in the presence of active nucleation sites.

(5) The experimentally determined superheat values ΔT_{mc} over a wide range of bath temperatures, from 2.31 to 4.62 K, are found to be in excellent agreement with the predictions of the homogeneous-nucleation theory [Eq. (2)]. This is discussed in greater detail in Sec. VI.

(6) Similar transient superheating experiments which we performed using platinum wire in liquid nitrogen and oxygen are consistent with the observations in liquid helium.²⁹ Excellent agreement with theory has been observed in all cases over a wide range of bath pressures. Moreover, the incep-

tion of nucleation in the case of liquid nitrogen was studied using laser scattering and acoustic transducers. The results obtained from these studies are consistent in almost all respects with the liquid-helium studies. We found a strong correlation between the inception of heterogeneous nucleation and the deviation of the observed transient superheat temperature from the predicted response on the basis of the thermal conduction assumption. In addition, the laser scattering experiments in liquid nitrogen are consistent with the sudden onset of nucleation at the sharp temperature overshoots. The results of the transient superheating experiments in liquid nitrogen provide us with a nonmagneto-resistive thermometry corroboration of the experimental technique.

(7) The fact that the observed constant superheat ΔT_{mc} does, in fact, represent the homogeneous nucleation superheat temperature, which is not affected by background radiation or cosmic rays, can be inferred from the lack of random fluctuations in ΔT_{mc} . To further validate this assumption, we subjected the heater surface to x rays from a radioactive source (²⁴¹Am) placed in close proximity to the heater surface. The same value of superheat ΔT_{mc} , at any given bath temperature, could be produced exactly but at slightly higher heating rates than normal.

(8) Questions may be raised regarding a possible effect of the external magnetic field, used in our thermometry technique, on the measured superheat temperature ΔT_{mc} . Because liquid helium is slightly diamagnetic compared to helium vapor, an applied magnetic field may possibly influence the measured homogeneous-nucleation temperature of liquid helium. This effect would be due to the difference in the magnetostatic energy in the liquid and the vapor nuclei in the presence of a magnetic field.²⁹ This energy difference causes a reduction in the pressure inside critical vapor nuclei, which then acts to increase the height of the thermodynamic barrier slightly, and consequently, raises the homogeneous-nucleation temperature. The estimated effect on the temperature turns out to be less than 1 μ K. An experimental check on this was made by repeating the transient superheating experiments at different magnetic fields. Changing the magnetic field from 0.4 to 1.5 T did not produce any detectable change in the observed maximum superheat ΔT_{mc} . Therefore, we conclude that the effect of the magnetic field is insignificant.

In summary, we feel that the points presented above constitute a convincing argument that the sharp peaks are due to a sudden onset of homogene-

ous nucleation in the superheated liquid layer in contact with the heater surface. Consequently, the superheat temperature ΔT_{mc} corresponding to the sharp peaks experimentally defines the homogeneous-nucleation limit in liquid ${}^4\text{He}$. Comparison of ΔT_{mc} with the theoretical predictions of the homogeneous-nucleation limit, derived from the BD theory [Eq. (2)], is presented in Sec. VI.

VI. ${}^4\text{He}$ NUCLEATION TEMPERATURE

In this section, we present the results of the homogeneous-nucleation-temperature measurements in liquid ${}^4\text{He}$. The measurement of the maximum superheat temperature ΔT_{mc} (see Fig. 2) are shown in Fig. 3 (solid triangles) as a function of HeI bath temperature T_b from 2.31 to 4.62 K. The ΔT_{mc} decreases with increasing temperature and is expected to vanish at the critical point. The solid line in Fig. 3 corresponds to the theoretical estimates of the homogeneous-nucleation temperature T_h ($T_h = \Delta T_h + T_b$, where ΔT_h is the superheat temperature) of ${}^4\text{He}$ as determined from Eq. (2).³⁰ In estimating T_h , we have assumed the nucleation rate to be equal to one critical nucleus/cm³s. This value of J was selected somewhat arbitrarily. Any error involved in the estimate is insignificant due to the extreme insensitivity of T_h to the assumed nucleation rate, as discussed in Sec. II.

The experimental data shown in Fig. 3 can be expressed in terms of the bath temperature by a single power law of the following form:

$$\Delta T_{mc} = 4.322(1 - T_b/T_c)^{1.534}, \quad (4)$$

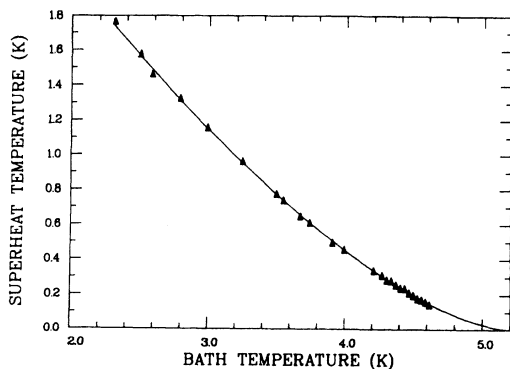


FIG. 3. Maximum superheat temperature as a function of bath temperature. The maximum superheat temperature ΔT_{mc} (solid triangles) is plotted as a function of bath temperature. The solid line represents the theoretical predictions of the homogeneous-nucleation temperature T_h , derived from Eq. (2), for a nucleation rate of $J=1$ critical nucleus/cm³s.

where T_c is the critical temperature of ${}^4\text{He}$. In terms of the reduced bath pressure P/P_c , the data can be presented as

$$T_{mc}/T_c = 0.753 + 0.224P/P_c, \quad (5)$$

with a standard deviation of 3 mK. Here, $T_{mc} = \Delta T_{mc} + T_b$, and P_c is the critical pressure of ${}^4\text{He}$. As Eq. (5) indicates, T_{mc} varies linearly with P .

In Sec. V, we presented a series of arguments to justify that ΔT_{mc} represents the homogeneous-nucleation superheat limit ΔT_h in liquid ${}^4\text{He}$. As can be seen from Fig. 3, the agreement between the ΔT_{mc} measurements and the predictions from the nucleation theory [Eq. (2)] is excellent over the entire experimental range. Such an agreement between experiment and theory reflects the adequacy of the conventional nucleation theory in describing the liquid-to-vapor nucleative phase transitions in a quantum system such as liquid ${}^4\text{He}$ (at least, far from the critical region).

In Fig. 3, we have extrapolated the theoretical predictions up to the critical point; however, nucleative behavior in the critical region may be modified from that predicted by either the BD theory [Eq. (2)], or the recent, more detailed hydrodynamic treatment by Langer and Turski (LT).¹⁴ The predictions of LT are quantitatively almost identical to those of the BD theory; however, there is no experimental confirmation of either of the above nucleation theories in the critical region. Experimental measurements of the homogeneous-nucleation limit in the critical region, for both binary mixtures and pure liquids, are found to exceed the predicted value by factors of 2 or more,³⁻¹⁰ although, one would expect the conventional nucleation theory to be most accurate in this situation.¹² Perhaps the crucial point here is that the nucleation rate is not measured directly in any of these experiments. Rather the usual procedure of experimentally defining the homogeneous-nucleation limit consists of observing the so-called cloud point, the point at which the number density of droplets and their sizes are big enough to allow visual observation. As first pointed out by Binder and Stauffer,¹¹ to describe this cloud-point phenomenon, it is clearly not enough to know only the nucleation rate. One also needs to consider the dynamics of the droplet growth, how fast the droplets grow once they are created. The discrepancy with theory may result because the growth of droplets is controlled by diffusion, and diffusive processes over critical length scales become very slow near the critical point.

The present transient superheating experiment in

^4He does not rely on visual observation of the homogeneous-nucleation limit. Here, the process of rapid formation of critical-size vapor bubbles in the superheated liquid layer is detected almost instantaneously because of the fast response time of the bismuth thermometer. Although the subsequent growth of the vapor bubbles can be followed through the temperature drop of the thermometer, caused by the energy consumed in the bubble growth process, the initial temperature at which the nucleation rate first becomes significant can be determined sufficiently accurately for quantitative comparison with theoretical predictions. Moreover, since these measurements are carried out far from the critical region, the growth rates are sufficiently high. This is so primarily because, in a liquid-vapor system, in contrast with binary mixtures, mass can be transferred from one place to another rapidly by kinetic and hydrodynamic flow instead of slowly by diffusion. Thus, we believe our measurements constitute a good test of the validity of the BD theory in the case of liquid ^4He . Moreover, as we discussed in Sec. II, there is no need to invoke a new nucleation mechanism, such as quantum tunneling, to explain homogeneous nucleation for positive bath pressures in superheated liquid helium I. Such tunneling nucleation is likely to be observed, if at all, only in tensile strength experiments. However, the observed disagreement between experiment and theory in case of tensile strength experiments in superfluid ^4He cannot be explained in terms of quantum nucleation because all these experiments were performed much above the tunneling temperature T^* , which we estimate to be approximately 0.3 K (see Sec. II). It would be interesting to study the effects of tunneling nucleation at temperatures < 0.3 K.

VII. CORRESPONDING-STATES ANALYSIS

Phenomenological analyses based on the principle of corresponding states have shown that this concept provides a useful method for systematizing the measured properties of one or more substances to predict the properties of other substances. In this section, we examine the homogeneous-nucleation-temperature measurements in ^4He (this work), along with similar measurements in Ar, Kr, Xe, and H_2 from other investigators,^{16,31} from the viewpoint of corresponding states. We show how, using this analysis, prediction of homogeneous-nucleation temperature can be made for hydrogen isotopes such as HD, DT, T_2 , and D_2 .

In Fig. 4, homogeneous-nucleation-temperature T_h measurements for H_2 and several noble gases are presented in terms of their scaled temperature T_h/T_c and bath pressure P/P_c , where T_c and P_c are the critical temperature and pressure, respectively: ^4He data from this work; Ar, Kr, and Xe data from recent capillary boiling experiments of Skripov *et al.*¹⁶; and H_2 data from bubble-chamber nucleation experiments by Hord *et al.*³¹ The H_2 data shown correspond to the maximum nucleation pressure at a given temperature. The solid lines are the theoretical predictions for each liquid determined from the homogeneous-nucleation theory, Eq. (2). The dashed line represents the van der Waals spinodal, shown here only as a qualitative reference line.

Note that all the experimental T_h data for the classical monatomic liquids such as Ar, Kr, and Xe fall on the same line, clearly demonstrating a corresponding-states type of behavior. The deviations from this line of both experimental data and theoretical predictions for the quantum liquids H_2 and ^4He are obviously due to quantum effects. Because no experimental data are available for ^3He , only the theoretical predictions are shown in Fig. 4. The magnitude of the deviations from the classical behavior is clearly dependent on the magnitude of the de Boer quantum parameter Λ [$\Lambda = h / \sigma(m\epsilon)^{1/2}$, where h is Planck's constant, m is the atomic mass, and ϵ and σ are the Lennard-Jones parameters representing, respectively, the strength and range of the interatomic potential].

The quantum effects on the homogeneous-nucleation temperature are better illustrated in Fig. 5 in which the temperature T_h and the pressure P are reduced using the Lennard-Jones parameters as $T_h^* = kT_h / \epsilon$ and $P^* = P\sigma^3 / \epsilon$. The significance of the dashed lines in the figure will be discussed later. Since the theoretical predictions for both classical and quantum liquids are obtained from the same nucleation theory rate expression (2) and these predictions are in excellent quantitative agreement with the experimental data, one can be reasonably sure that the quantum effects are not due to some additional quantum mechanism of nucleation, such as quantum tunneling (see Sec. VI).

The source of the quantum effect becomes apparent if we recast the nucleation-rate expression (2) in terms of reduced (dimensionless) quantities as follows:

$$\begin{aligned} J^* &= J\sigma^4 \sqrt{(m/\epsilon)}; \quad \gamma^* = (\sigma^2/\epsilon)\gamma, \\ N^* &= N\sigma^3; \quad t^* = (\epsilon/m\sigma^2)^{1/2}t. \end{aligned} \quad (6)$$

With the above reduced quantities, the rate expression becomes

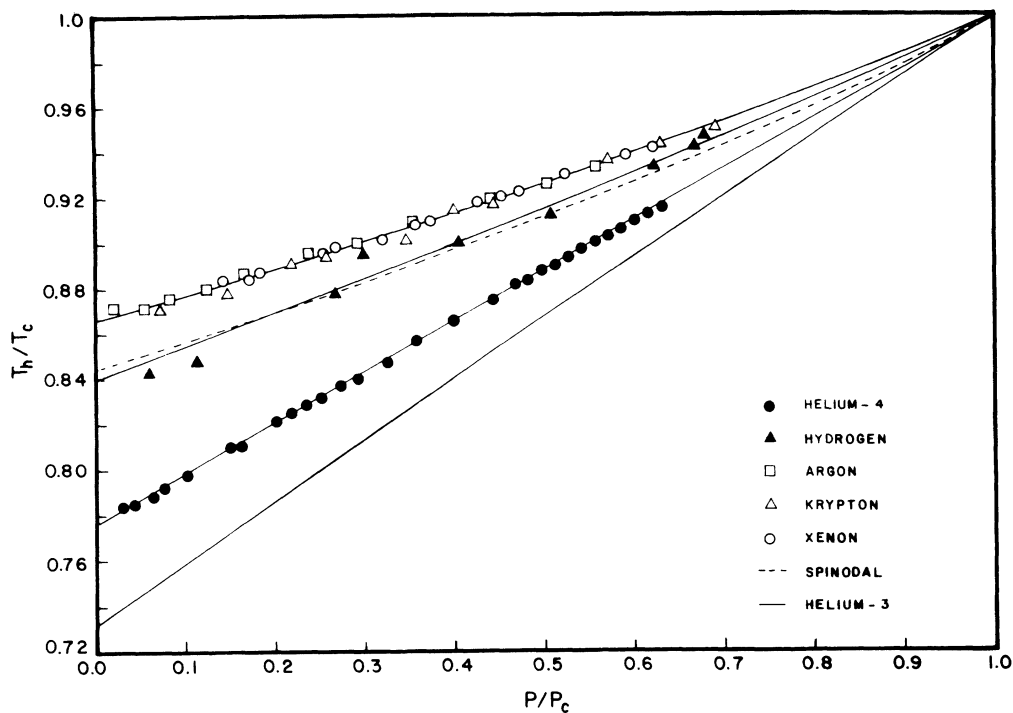


FIG. 4. Scaled homogeneous-nucleation temperature T_h/T_c vs scaled pressure P/P_c . The homogeneous-nucleation-temperature data are presented as a function of the bath pressure for Ar, Kr, Xe, H₂, and ⁴He. The solid lines represent the theoretical predictions of T_h from Eq. (2) for each liquid. The van der Waals spinodal is shown by the dashed line.

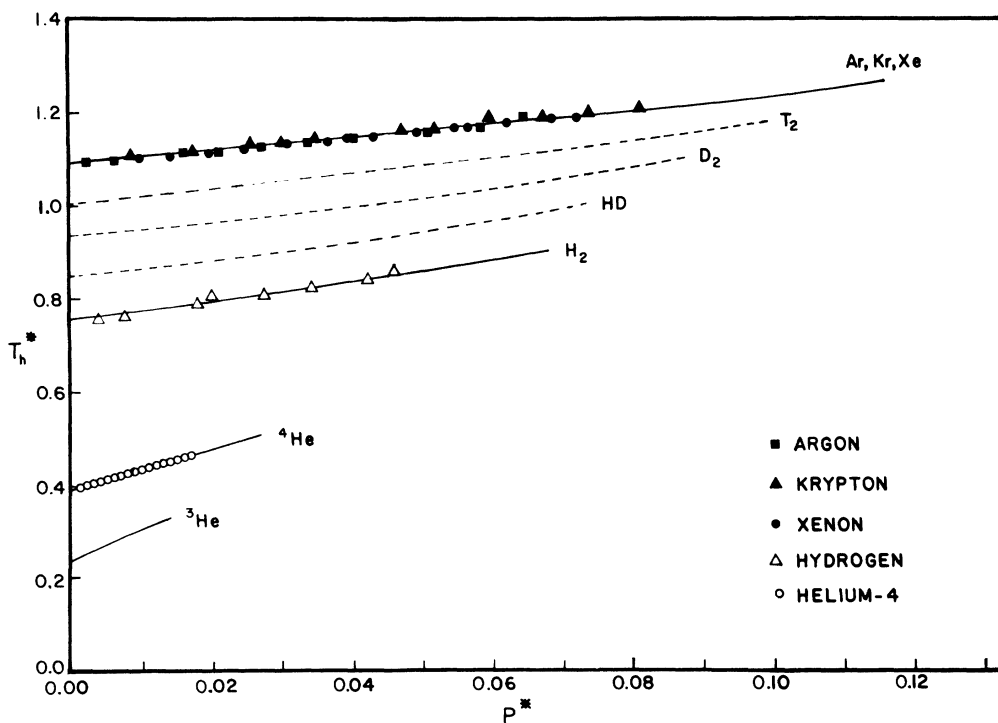


FIG. 5. Reduced homogeneous-nucleation temperature T_h^* vs reduced pressure P^* . The data shown in Fig. 4 are reduced according to Eq. (12) and are presented here. The dashed lines are the predictions of the homogeneous-nucleation temperatures for the hydrogen isotopes T₂, D₂, and HD.

$$J^* = N^* \left[\frac{2\gamma^*}{\pi B} \right]^{1/2} \exp \left[- \frac{16\pi\gamma^*{}^3}{3T^*(P_V^* - P_L^*)^2} \right], \quad (7)$$

where J^* is the number of critical nuclei per unit reduced time and volume. Because thermophysical properties such as surface tension, vapor pressure, etc., for the classical monatomic liquids Ar, Kr, and Xe obey the classical corresponding-states-type behavior rather well,³² these liquids should have the same reduced homogeneous nucleation temperature T_h^* at any given reduced bath pressure P^* (or bath temperature). This is indeed true and can be seen from Fig. 5. It is obvious that since the reduced bulk properties of H_2 , 4He , and 3He deviate significantly from those of Ar, Kr, and Xe,³² the reduced nucleation temperatures as derived from Eq. (7) also should deviate accordingly. One can effectively incorporate these quantum effects in the rate expression (7) through the thermophysical properties in terms of Λ , such as $\gamma^*(\Lambda)$,³³ $P^*(\Lambda)$, etc. We, however, take a simpler approach to illustrate the quantum effects on the corresponding-states behavior of homogeneous nucleation.

We find that the available nucleation data for both classical and quantum liquids can be quite satisfactorily correlated by an expression of the form

$$(1 - T_h/T_c) = m(\Lambda)(1 - P/P_c)^{n(\Lambda)}, \quad (8)$$

which provides an explicit relationship between the homogeneous-nucleation temperature and the saturation bath pressure. The parameters m and n , respectively, describe the slope and the curvature of the lines representing the nucleation data in Fig. 4, and we have assumed these parameters to be dependent Λ . Interestingly, the curvature parameter n for 4He is 1.001, indicating a linear relationship between T_h and P . The parametric dependence of m and n on Λ is shown in Fig. 6. The values of the parameters m and n for all liquids considered here were determined from a nonlinear least-squares-curve fit of the predicted homogeneous-nucleation temperatures evaluated by using Eq. (2) for a nucleation rate of $J=1$. Because the nucleation data used in our analysis here are from radically different experimental techniques, the associated nucleation rates are different. Consequently, we standardize our correlation by arbitrarily selecting a reference value of $J=1$ and using the theoretical values instead of the experimental data. Any error from this process is very small, due to the insensitivity of the homogeneous-nucleation temperature to the nucleation rate J .

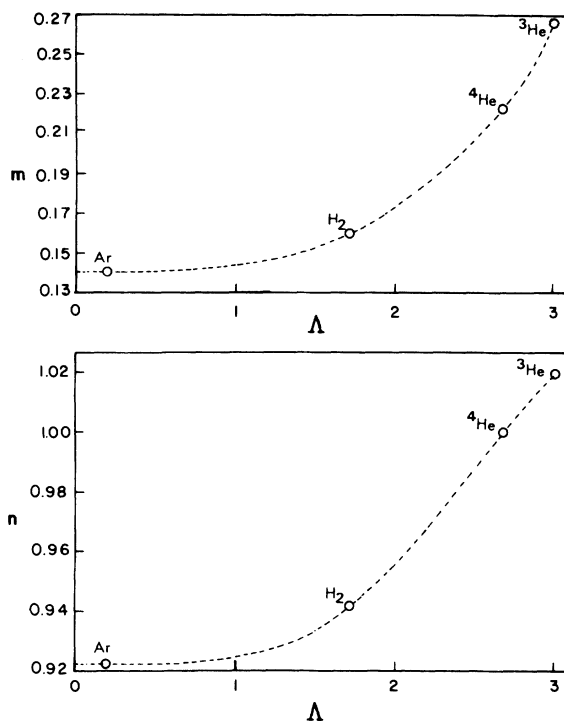


FIG. 6. Plot of Eq. (15). Λ is the de Boer parameter. The circles represent the values for the parameters m and n for Ar, H_2 , 4He , and 3He .

The parameters m and n can be fitted as a series in powers of Λ^2 as

$$m(\Lambda) = \sum_{l=0}^j a_l \Lambda^{2l}, \quad n(\Lambda) = \sum_{l=0}^j b_l \Lambda^{2l}. \quad (9)$$

The predominant contributions to m and n in Eq. (9) arise through the first few terms. The result of employing the first four coefficients a_l and b_l are tabulated in Table I. These coefficients were determined from the values of m and n for Ar, H_2 , 4He , and 3He . Although hydrogen is diatomic, we have included it in our analysis because its interatomic potential can be assumed to be approximately spherically symmetric.³⁴ This is due to the fact that

TABLE I. Values of the first four coefficients a_l and b_l appearing in Eq. (15).

l	a_l	b_l
0	0.14037	0.92185
1	1.8239×10^{-3}	-1.9990×10^{-4}
2	1.8450×10^{-3}	2.9165×10^{-3}
3	-6.6426×10^{-5}	-1.9062×10^{-4}

the population of excited rotational states of para H_2 below the critical temperature is low, inelastic collisions are essentially nonexistent, and a spherically symmetric force field is, therefore, approximately applicable. We know that the deviations of the T_h^* -vs- P^* curves for the quantum liquids from the single curve representing the classical fluids (see Fig. 5) are due to the quantum effects not included in the reduced quantities in Eq. (6). If Λ is incorporated as a scaling unit, in addition to the two Lennard-Jones parameters ϵ and σ in reducing the physical variables, a single curve should represent the behavior of both the classical and the quantum liquids. A simple and straightforward way to accomplish this latter result would be to use Eq. (8) to define two quantum variables containing Λ as

$$\Gamma = (1 - T_h/T_c)/m(\Lambda)$$

and (10)

$$\Pi = (1 - P/P_c)^{n(\Lambda)},$$

where $m(\Lambda)$ and $n(\Lambda)$ are obtained using Eq. (9) and the values of Table I. The new variables Γ and Π are now functions of Λ and, therefore, Eq. (8) simply becomes $\Gamma(\Lambda) = \Pi(\Lambda)$. This constitutes a statement of an empirical law of corresponding states for the homogeneous-nucleation temperature in both classical and quantum liquids. Figure 7 il-

lustrates the universal curve that results when Eq. (10) is employed for the homogeneous-nucleation temperature. As expected, we find that a single straight line in the Γ - Π plane satisfactorily represents the nucleation data for all the liquids considered here, including the quantum liquids. The slight deviation of the data for Ar, Kr, and Xe is due to the differences in the experimental nucleation rates as mentioned earlier.

An obvious use of the quantum-mechanical law of corresponding states is for predicting T_h for several hydrogen isotopes. Knowledge of the reduced pressure and Λ is sufficient to predict accurately T_h of any hydrogen isotope. For this, a useful form of Eq. (8) is

$$T_h^* = T_c^* [1 - m(\Lambda)(1 - P^*/P_c^*)^{n(\Lambda)}], \quad (11)$$

where m and n are given by Eq. (9) or can be obtained from Fig. 6. The dashed lines in Fig. 5 represent the predictions of T_h for D_2 , HD , and T_2 . It is otherwise difficult to obtain theoretical values for T_h for these substances simply on the basis of the nucleation theory because the required thermo-physical properties are not readily available, e.g., no surface tension data are available for T_2 . In the interest of clarity, we have not included in Fig. 6 the prediction for DT , for which the values of the parameters m and n are 0.1457 and 0.9263, respec-

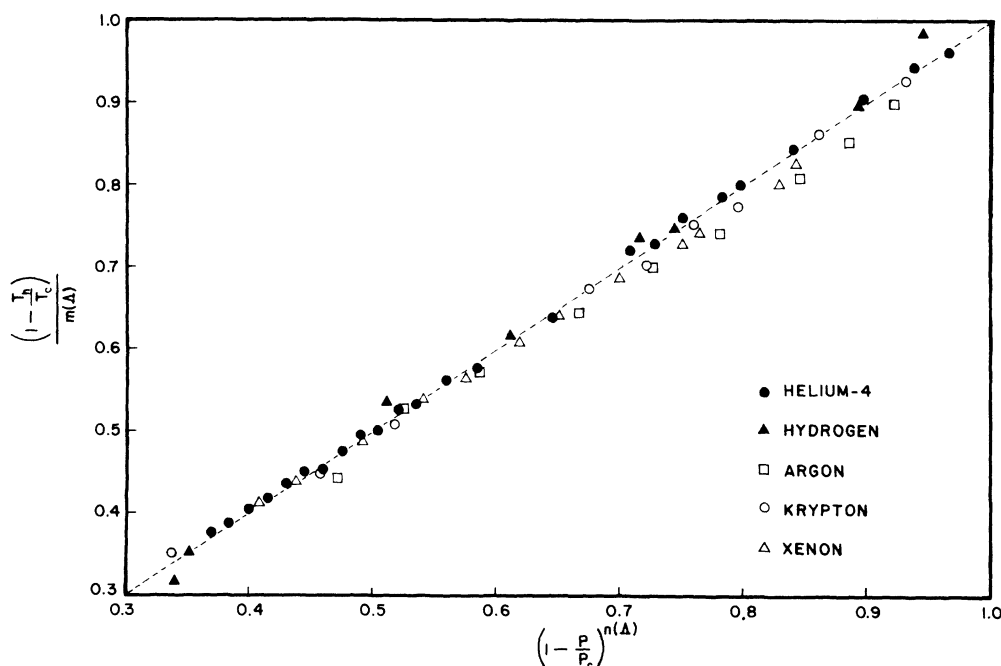


FIG. 7. Universal curve for the homogeneous-nucleation temperatures of liquid noble gases. The dashed line is a plot of Eq. (16).

tively. The values of Λ used in the predictions for the heteronuclear isotopes HD and DT have been computed after Friedman.³⁵

Finally, we would like to comment on the possible modification of Eq. (11) in the critical region. In the LT hydrodynamic model of nucleation near the critical point,¹⁴ the essential parameters, such as the thermophysical properties of the system, are expressed in simple scaling forms in terms of the appropriate critical exponents. Since in the critical region the thermophysical properties of both classical and quantum liquids can be described by the same critical exponents, one may expect that our empirical expression (11), which expresses the results of the nucleation-rate equation (2) and which in turn depends on the thermophysical properties of the liquid, should be modified such that $n(\Lambda) \rightarrow n(0)$ as the critical point is approached. It would be interesting to study homogeneous nucleation in liquids ^3He and ^4He near and within the asymptotic critical region in order to study this quantum crossover effect. The very limited data by Dahl and Moldover⁷ in ^3He near the critical point is consistent with the above picture,¹³ although no definite conclusion regarding the validity (or lack thereof) of the BD theory in the critical region can be drawn from their data.

VIII. SUMMARY

We have presented experimental data on homogeneous nucleation in liquid helium I over a large temperature range, far from the critical point. We find excellent agreement of our data with the predictions from Becker-Döring nucleation theory over the entire temperature range studied. Such agreement has not been observed in tensile strength experiments in liquid ^4He . Our data clearly demonstrate the adequacy of the conventional nucleation theory in describing the first-order, thermally ac-

tivated transition kinetics in a quantum liquid, such as liquid ^4He . This is consistent with the quantum theory of nucleation, first proposed by Lifshitz and Kagan,¹⁹ in which they showed that, at temperatures above ~ 0.3 K, the nucleation mechanism is thermal activation over the thermodynamic barrier in metastable liquid helium. Subbarrier tunneling transitions become probable only at temperatures below ~ 0.3 K.

When our helium data are compared with nucleation data in Ar, Kr, Xe, and H_2 in terms of reduced temperature and pressure, we find significant quantum deviations of the ^4He and H_2 data from a corresponding-states type of behavior, which is otherwise obeyed well by the classical monatomic liquids. We believe these deviations to be due to quantum effects on the bulk thermophysical properties of the liquids. The deviations of the quantum liquids from classical behavior are found to be parametrically dependent on the de Boer quantum parameter Λ and this has enabled us to predict the homogeneous-nucleation temperatures for several hydrogen isotopes. We have also included theoretical predictions for ^3He in our corresponding-states analysis.

ACKNOWLEDGMENTS

We are grateful to Dr. W. E. Keller for his critical comments on this paper. We have benefitted from useful discussions with Dr. Makoto Takeo. We wish to thank L. Thannum and B. McLaughlin for their assistance with the electronics, and J. Janacek and R. Zupan for constructing the mechanical devices. This work was carried out at the Physics Department, Portland State University, in partial fulfillment of the requirements for the Ph.D. degree by one of us (D.N.S.). Partial support for this work was provided by the U.S. Department of Energy.

¹R. Becker and W. Döring, *Ann. Phys. (Leipzig)* **24**, 719 (1935).

²See, for example, J. Frenkel, *Kinetic Theory of Liquids* (Dover, New York, 1955); *Nucleation*, edited by A. C. Zettlemoyer (Dekker, New York, 1969); *Nucleation Phenomena*, edited by A. C. Zettlemoyer (Elsevier, New York, 1977).

³B. E. Sundquist and R. A. Oriani, *J. Chem. Phys.* **36**, 2604 (1962).

⁴R. B. Heady and J. W. Cahn, *J. Chem. Phys.* **58**, 896

(1973).

⁵S. Krishnamurty and W. I. Goldberg, *Phys. Rev. A* **22**, 2147 (1980).

⁶J. S. Huang, W. I. Goldberg, and M. R. Moldover, *Phys. Rev. Lett.* **34**, 639 (1975).

⁷David Dahl and M. R. Moldover, *Phys. Rev. Lett.* **27**, 1421 (1971).

⁸A. J. Schwartz, S. Krishnamurty, and W. I. Goldberg, *Phys. Rev. A* **21**, 1331 (1980).

⁹J. S. Huang, S. Vernon, and N. C. Wong, *Phys. Rev.*

- Lett. 33, 140 (1974).
- ¹⁰Rebekah G. Howland, Ning-Chong Wong, and Charles M. Knobler, *J. Chem. Phys.* 73, 522 (1980).
- ¹¹K. Binder and D. Stauffer, *Adv. Phys.* 25, 343 (1976).
- ¹²J. S. Langer and A. J. Schwartz, *Phys. Rev. A* 21, 928 (1980).
- ¹³K. Binder, *J. Phys.* 41, C4–51 (1980).
- ¹⁴J. S. Langer and L. A. Turski, *Phys. Rev. A* 8, 3230 (1973).
- ¹⁵See, for example, M. Blander, *Adv. Colloid Interface Sci.* 10, 1 (1979); M. Blander and J. L. Katz, *AIChE J.* 21, 853 (1975).
- ¹⁶V. P. Skripov, V. G. Baidakov, and A. M. Kaverin, *Physica (Utrecht)* 95A, 169 (1979).
- ¹⁷J. W. Beams, *Phys. Fluids* 2, 1 (1959).
- ¹⁸P. L. Marston, *J. Low Temp.* 25, 383 (1976).
- ¹⁹I. M. Lifshitz and Y. Kagan, *Zh. Eksp. Teor. Fiz.* 62, 385 (1972) [*Sov. Phys.—JETP* 35, 206 (1972)].
- ²⁰Yu. Kagan, *Russ. J. Phys. Chem.* 34, 42 (1960).
- ²¹F. F. Abraham, *Homogeneous Nucleation Theory* (Academic, New York, 1974).
- ²²L. C. Brodie, Dipen N. Sinha, J. S. Semura, and C. E. Sanford, *J. Appl. Phys.* 48, 2882 (1977); L. C. Brodie, D. N. Sinha, C. E. Sanford, and J. S. Semura, 99th American Society of Mechanical Engineers Winter Annual Meeting, San Francisco, 1978.
- ²³L. C. Brodie, Dipen N. Sinha, C. E. Sanford, and J. S. Semura, *Rev. Sci. Instrum.* 52, 1697 (1981).
- ²⁴E. Oker and J. Merte, Jr., *Proceedings of the 6th International Heat Transfer Conference, Part I, Toronto, 1978* (Hemisphere, Washington, D.C., 1979), Vol. 5, p. 139.
- ²⁵Y. Y. Hsu and R. W. Graham, NASA Technical Note No. D-594 (1961); C. Y. Han and P. Griffith, *Int. J. Heat Mass Transfer* 8, 887 (1965).
- ²⁶See, for example, V. P. Skripov, *Metastable Liquids* (Wiley, New York, 1974).
- ²⁷L. J. Rybarczyk and J. T. Tough, *J. Low Temp. Phys.* 43, 197 (1981).
- ²⁸H. Lurie and H. A. Johnson, *J. Heat Transfer* 84, 217 (1962).
- ²⁹Dipen N. Sinha, Ph.D. thesis, Portland State University, 1980 (unpublished).
- ³⁰The surface tension values used in estimating T_h are based upon an interpolation of the measurements of J. F. Allen and A. D. Misener, *Proc. Camb. Phil. Soc.* 34, 299 (1938). More recent measurements by D. P. E. Dickson, D. Caroline, and E. Mendoza, *Phys. Lett.* 33A, 139 (1970) and P. J. King and A. F. G. Wyatt, *Proc. R. Soc. London, Ser. A* 322, 355 (1971) are in excellent agreement with the earlier measurements of surface tension of helium I of Allen and Misener. Other thermophysical properties are taken from R. D. McCarty, *J. Phys. Chem. Ref. Data* 2, 923 (1973).
- ³¹J. Hord, R. B. Jacobs, C. C. Robinson, and L. L. Sparks, *Trans. ASME* A86, 485 (1964).
- ³²See, for example, Ludwig Bewilogua and Christel Gladun, *Contemp. Phys.* 9, 277 (1968).
- ³³Dipen N. Sinha, J. S. Semura, and L. C. Brodie, *J. Chem. Phys.* 76, 2028 (1982).
- ³⁴J. D. Rogers and F. G. Brickwedde, *Physica (Utrecht)* 32, 1004 (1966).
- ³⁵H. Friedman, *Advances in Chemical Physics* (Interscience, New York, 1962), Vol. IV.